ORGANOMETALLICS

pubs.acs.org/Organometallics Article

To Bind or Not to Bind: Mechanistic Insights into C–CO_2 Bond Formation with Late Transition Metals

Diego García-López, Ljiljana Pavlovic, and Kathrin H. Hopmann*

Cite This: https://dx.doi.org/10.1021/acs.organomet.0c00090 Read Online

ACCESS | Metrics & More | Article Recommendations | Supporting Information

ABSTRACT: In transition metal-mediated carboxylation reactions, CO_2 inserts into a metal–nucleophile bond. At the carboxylation transition state (TS), CO_2 may interact with the metal (*inner*-sphere path) or may insert without being activated by the metal (*outer*-sphere path). Currently, there is no consensus as to which path prevails. In order to establish general predictions for the insertion of CO_2 into metal–carbon bonds, we computationally analyze a series of experimentally reported Cu, Rh, and Pd complexes. Our focus is on carboxylation of aromatic substrates, including C_{sp^3} *benzyl* and C_{sp^2} *aryl* and *alkenyl* nucleophiles. We observe clear trends, where the nature of the nucleophile determines the preferred path: benzylic C_{sp^3} nucleophiles favor *outer*-sphere and C_{sp^2} systems favor *inner*-sphere CO_2 insertion into the metal–carbon bond. An exception are Cu–benzyl bonds, where *inner*- and *outer*-sphere CO_2 insertions are found to be competitive, highlighting the need to include both paths in mechanistic studies and in the rationalization of experimental results. For insertion into Pd–C_{sp^2} bonds, we find that the metal–CO_2 interactions at the TS are weak and may be beyond 3 Å for sterically congested ligands. Nonetheless, on the basis of a comparison to other TSs, we argue that the CO_2 insertion into Pd–C_{sp^2} bonds should be classified as *inner*-sphere.

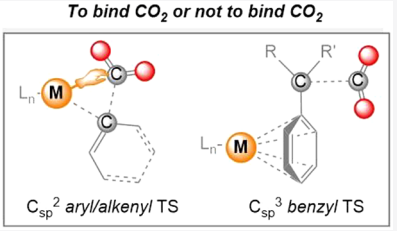

INTRODUCTION

Carbon dioxide has the potential to become a versatile building block in organic synthesis.[1−6] Carboxylation of organic molecules with CO_2 can be catalyzed by transition metals, with good yields for a wide variety of compounds.[1,2,6] A number of mechanistic studies have been performed on metal-mediated C–CO_2 bond formation,[7−22] and on the basis of these, the observed mechanisms can be divided into two classes:[23,24] those that involve metal–CO_2 interactions at the C–C bond formation transition state (TS, *inner*-sphere pathways) and those that do not (*outer*-sphere pathways, Figure 1).

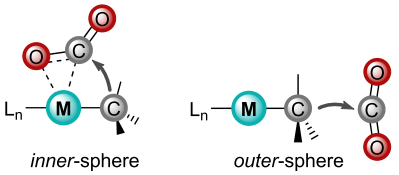

Figure 1. Mechanisms for C–CO_2 bond formation.

Knowledge about the intimate behavior of CO_2 during C–C bond formation is of importance for at least two reasons. First, as CO_2 is an inert molecule, it may be expected that metal–CO_2 interactions at the TS are needed to polarize and activate CO_2.[25] The lack of such interactions would then render CO_2 less active. Interestingly, for some CO_2 hydrogenations, where mechanistic studies predicted an *outer*-sphere path, it has been shown that Lewis acid additives enhance the reaction rate, possibly by binding and activating the free CO_2 molecule.[26] Insights into the intrinsic behavior of CO_2 can thus help to rationalize and predict the effect of additives. Second, in carboxylations involving prochiral nucleophiles, the configuration of the generated chiral center may depend on the mode of CO_2 insertion. Once the diastereomeric metal–nucleophile intermediate is formed, *inner*-sphere CO_2 insertion would retain a given configuration, whereas *outer*-sphere insertion would prompt an inversion. It is relevant to note that there have been relatively few asymmetric C–CO_2 bond formations reported,[6,27−30] often with low to medium enantiomeric excesses (ee's). It is tempting to speculate that the low ee's in some cases may originate from the inability to restrict the CO_2 molecule to one of the two possible insertion paths. An understanding of how CO_2 behaves could support the design of systems that clearly favor one insertion mode, resulting in better enantioselectivities.

To date, there is no clear consensus as to which pathway, *inner* or *outer*, generally is preferred for C–CO_2 bond formation with late transition metals. For sp^2 and benzylic sp^3 nucleophiles, various complexes based on e.g. Cu, Rh, or Pd have been studied computationally, and it was concluded

Received: February 9, 2020

that these systems proceed via *inner*-sphere CO_2 insertion,[21,23,31−37] but alternative *outer*-sphere paths were not always tested. Actually, for Rh−COD-catalyzed C−C bond formation with benzylic substrates, we recently showed a strong preference for *outer*-sphere insertion.[7] A review on the behavior of group 9 and 10 metals in CO_2 insertion reactions with a variety of metal−X complexes (X = H, OR, NR_2, CR_3) concluded that systems with low nucleophilicity, including metal−alkyl nucleophiles, prefer *outer*-sphere paths.[24] However, only few metal−alkyl examples following this trend were identified, among them Ni and Pd complexes with allylic or nonbenzylic C_{sp^3} nucleophiles.[9−11] Unfortunately, for many computational studies, it is unclear if both CO_2 insertion modes were evaluated. Further, it is uncertain if the often encountered practice of truncating computational models may have an effect on the mechanistic outcome.

In this work, the prerequisite of a metal−CO_2 interaction for C−CO_2 bond formation is analyzed computationally for a series of experimentally reported examples involving late transition metals: Cu, Rh, and Pd. These metals represent groups 9−11, and they were chosen due to their successful performance in many C−CO_2 bond formations.[30,38−44] The selected examples also represent a variety of well-known ligands, with monodentate NHC, bidentate phosphine, or tridentate pincer ligands. Our focus is on C−CO_2 bond formation with aromatic substrates, including C_{sp^3} *benzyl* and C_{sp^2} *aryl* and *alkenyl* nucleophiles, with all calculations performed on full molecular models.

COMPUTATIONAL DETAILS

Models. All calculations were carried out employing full molecular models (Table S1), without truncations or symmetry constraints. A closed-shell description of the electronic structure was employed for all systems.

Computational Methods. Quantum mechanical calculations were performed within the framework of density functional theory (DFT)[45] by employing Gaussian 09, Rev. D01.[46] Unless specifically indicated otherwise, the B3LYP[47,48] functional and the Grimme empirical dispersion correction D3[49,50] and the implicit IEFPCM[51] solvent model were used for geometry optimizations to locate either minima or first-order saddle points (transition states). The nature of the stationary points encountered was characterized by means of harmonic vibrational frequency analysis. All transition metals were described with a Stuttgart/Dresden SDD basis set with the associated pseudopotential,[52,53] while the rest of the atoms were described with 6-31++G(d,p).[54−58] This basis set combination is here referred to as BS1.

Energies. Electronic single point energies were computed with basis set BS2, comprising 6-311++G(2d,2p)[57,59−61] (nonmetal atoms) and SDD(f)[62] (metal atoms). Temperature corrections (T_{corr}) were applied in order to match the experimental reaction conditions. The final Gibbs free energies (1 atm standard state) are computed as

$$G = G_{BS1} - E_{BS1} + E_{BS2} + T_{corr}$$

Free energy barriers ($\Delta G^{\ddagger}$) for the CO_2 insertion TSs are calculated relative to a reactant state composed of the metal−alkyl and free CO_2.

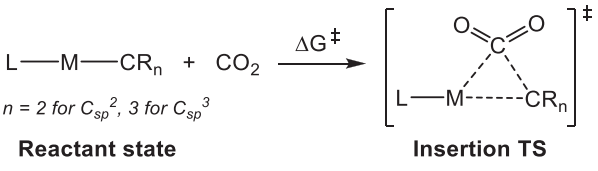

For Rh−C_{sp^2} systems, a metal−(alkyl)(CO_2) adduct was more stable than the reactant with free CO_2; in this case, barriers are calculated with respect to the adduct.

RESULTS AND DISCUSSION

From the literature, we selected Cu, Rh, and Pd complexes that were reported to promote CO_2 insertion into metal−C_{sp^3} or −C_{sp^2} bonds. In order to be able to isolate the effect of the carbon nucleophile on the CO_2 insertion path, complexes with similar ligands were chosen for the two kinds of nucleophiles. A compilation of studied reactions is given in the Table S1 in the Supporting Information. The following discussion is structured on the basis of the studied metal, with a subdivision based on the type of nucleophile, *benzyl* or *aryl*/*alkenyl*.

Copper-Based Benzylic C_{sp^3} Nucleophiles. The coupling of diborane compounds with CO_2 in the presence of Cu can lead to selective boracarboxylation of alkynes,[63] alkenes,[38] and aldehydes.[64] The group of Popp and co-workers followed this strategy to functionalize vinylarenes employing NHCs as a Cu ligand to obtain single constitutional isomers.[38] The proposed mechanism involves the formation of a borylcuprate species that inserts the vinylarene into the Cu−B bond.[65] This step was proposed to be rate limiting and to determine the regioselectivity of the following carboxylation of the formed benzylic carbon.[36,65] In experiments, the NHC ligands IPr and IMes showed different performances, with observed yields of the desired carboxylation product of 17% and 85%, respectively.[38] Analysis of the carboxylation barriers with various NHCs pointed to the conclusion that both the electronic and steric natures of the NHC affect the nucleophilicity of the alkyl.[65] However, only *inner*-sphere CO_2 insertion was considered in the computational evaluations.[36,65]

Here we studied the *inner*- and *outer*-sphere CO_2 insertion into the Cu−benzyl intermediate formed in the carboxylation of styrene (Scheme 1).[38] Our computations include three

Scheme 1. Computed CO_2 Insertion Step in the Cu−NHC-Catalyzed Boracarboxylation of Styrene[a]

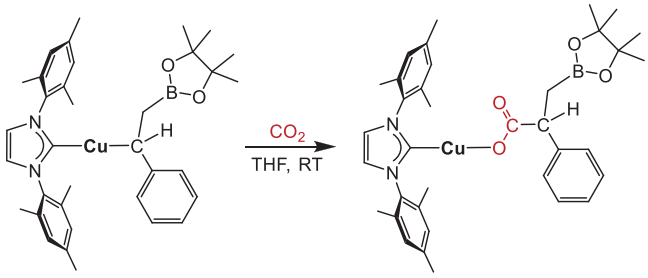

[a]The experimental reaction was originally reported in ref 38.

different NHCs: the experimentally studied IPr and IMes ligands[38] and the *N*-methyl analogue IMe, which has a reduced steric environment (Figures 2 and 3). The results show a substantial preference (2.5 kcal/mol) for *inner*-sphere carboxylation for the smallest IMe ligand, a weaker *inner*-sphere preference (1.3 kcal/mol) for IMes, and a preference for *outer*-sphere insertion (1.6 kcal/mol) for IPr, the largest ligand (Figure 2). The three studied NHCs can be assumed to have small differences in electron donation ability (with the order IMe < IMes ≤ IPr),[66] and therefore we suggest that the differences in barriers and insertion paths mainly should be

https://dx.doi.org/10.1021/acs.organomet.0c00090
Organometallics XXXX, XXX, XXX−XXX

	Cu-IMe	Cu-IMes	Cu-IPr
	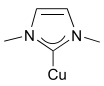	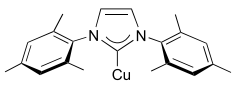	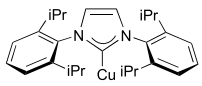
$\Delta G^{\ddagger}_{inner}$	16.4	18.8	22.0
$\Delta G^{\ddagger}_{outer}$	18.9	20.1	20.4

Figure 2. Computed barriers (kcal/mol, 298 K) for carboxylation of NHC−Cu−benzyl complexes.

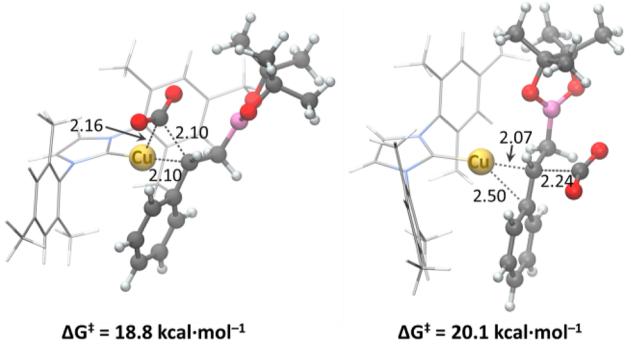

Figure 3. Optimized TSs for *inner*- (left) and *outer*-sphere (right) carboxylations of a benzylic intermediate in the Cu−IMes-catalyzed boracarboxylation (THF, 298 K). Distances are given in Å.

ascribed to sterics. It can be noted that, as the NHC ligand is enlarged, the barriers rise for both the *inner*- and the *outer*-sphere CO_2 insertions. The barrier increase caused by sterics is larger for *inner*-sphere insertion, which intuitively makes sense, eventually leading to preferred *outer*-sphere insertion.

In order to support the preference for *outer*-sphere CO_2 insertion for large NHC ligands, we find it instructive to discuss a related system. Recently, we investigated the Cu−IPr-mediated carboxylation of organoboranes,[67] a reaction originally reported by Skrydstrup, Nielsen, and co-workers.[39] This transformation involves a Cu−benzyl species, which inserts CO_2 (reaction 2 in Table S1 and Figure S1). In our earlier study, a full molecular model was evaluated with DFT (ωB97XD) and DLPNO-CCSD(T), including solvent and temperature (393 K) corrections. Both levels of theory favored an *outer*-sphere path, by respectively 1.8 and 0.3 kcal/mol. Here, we have repeated these calculations with the B3LYP-D3 protocol and again find a small preference for *outer*-sphere CO_2 insertion by 1.0 kcal/mol (393 K). The results obtained for CO_2 insertion into Cu−benzyl bonds are thus consistent across different computational models and methods.

The small differences in barrier for *inner*-sphere versus *outer*-sphere CO_2 insertion for NHC−copper−benzyl species indicate that both pathways are competitive in experiments. This leads to two important conclusions. First, for Cu−NHC complexes, both *inner*- and *outer*-sphere CO_2 insertion should always be evaluated in mechanistic studies. Second, Cu−NHC systems may not be promising for stereoselective carboxylations, because the competing *inner*- and *outer*-sphere TSs would provide opposite configurations. For example, the Cu−NHC-catalyzed bora- and hydrocarboxylations both form products with chiral centers (Scheme 1 and Table S1, reaction 2), making development of an asymmetric version of these reactions desirable.[38,39] However, even if a chiral NHC ligand may strongly favor one of the two diastereomeric Cu−benzyl intermediates, the subsequent CO_2 insertion would give low ee's, if both *inner*- and *outer*-sphere insertion takes place. For example, the barrier difference of 1.0 kcal/mol computed for reaction 2 (Table S1) would imply an ee of only 56% (393 K).[68]

Copper-Based Alkenyl and Aryl C_{sp^2} Nucleophiles. Cu−NHC-catalyzed hydrocarboxylation of alkynes to α,β-unsaturated carboxylic acids employing hydrosilane as a mild reducing agent was developed by Tsuji and co-workers (Scheme 2).[40] The authors reported that symmetric bis-

Scheme 2. Computed CO_2 Insertion Step in the Cu-Catalyzed Hydrocarboxylation of Alkynes[a]

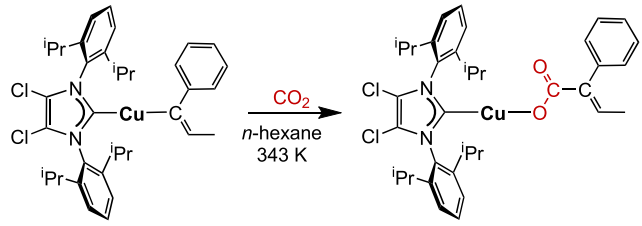

[a]The experimental reaction was originally reported in ref 40.

substituted acetylene derivatives afford the corresponding *E* isomers of the carboxylic acid. A proposed mechanism was analyzed computationally by means of DFT, employing a truncated catalyst.[34] The four computationally studied substrates all displayed the same regioselectivity, which was stated to be determined after the insertion of the alkyne substrate into the Cu−hydride bond of the active catalyst.[34] For the subsequent C−CO_2 bond formation, an *inner*-sphere path was reported.

We studied the carboxylation of the Cu−alkenyl intermediate computationally and succeeded in optimizing both the *inner*- and *outer*-sphere TSs with a full model, using Cl_2IPr as ligand and an alkenyl derived from 1-phenyl-1-propyne (Figure 4).[69] The angle of the CO_2 molecule at the *outer*-sphere

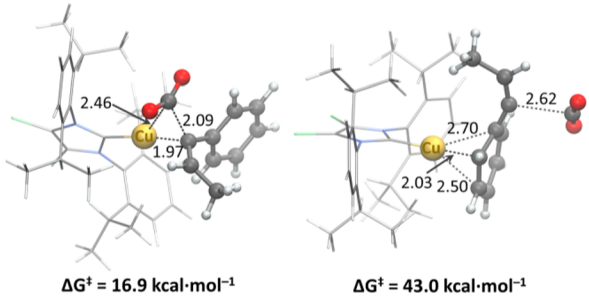

Figure 4. Optimized TS geometries for *inner*- (left) and *outer*-sphere (right) CO_2 insertion into a Cu−alkenyl intermediate (*n*-hexane, 343 K). Distances are given in Å.

(167°) and *inner*-sphere (144.5°) TS indicates that CO_2 is experiencing considerably more activation in the latter. The computed *outer*-sphere barrier of 43.0 kcal/mol is impossible to overcome at a reaction temperature of 70 °C, whereas 16.9 kcal/mol for the *inner*-sphere insertion should be very feasible (up to 29 kcal/mol may be considered viable[70]). It can be noted that the carboxylation barrier does not necessarily represent the overall reaction barrier, as other steps may be rate limiting. However, here we are concerned only with the preferred CO_2 insertion mode, and the results clearly show

https://dx.doi.org/10.1021/acs.organomet.0c00090
Organometallics XXXX, XXX, XXX−XXX

that, for this Cu−alkenyl species, the *inner*-sphere path is favored by 26.1 kcal/mol over *outer*-sphere insertion.

A Cu−IPr complex was also used by Hou and co-workers in the catalytic synthesis of arylcarboxylic acids from arylboronic esters (Table S1, reaction 4).[41] Also other organoboronic esters such as vinylic moieties were converted into the corresponding α,β-unsaturated acids. The mechanism was studied computationally by Marder, Lin, and co-workers,[32] and an *inner*-sphere TS was reported for a catalyst model, wherein the bulky IPr arms were replaced by Me groups. As shown above (Figure 2), such a truncation may affect the steric constraints and the preferred CO_2 insertion path. Therefore, we studied the full IPr ligand with two experimental substrates, 4-methoxyphenyl and 4-methoxystyrene (Table S1, reactions 4a,b, and Figure S2).[41] As for the truncated catalyst model, our computations on the full model provide the *inner*-sphere CO_2 insertion path for both the *aryl* and the *alkenyl* C_{sp^2} nucleophiles, with identical barriers of 15.2 kcal/mol (343 K). All attempts to obtain *outer*-sphere TSs for these systems failed. On the basis of the three examples discussed here, a strong preference for *inner*-sphere CO_2 insertion is apparent for Cu−IPr-mediated carboxylations of C_{sp^2} nucleophiles, which is in contrast to the dual pathways observed for benzylic C_{sp^3} nucleophiles.

Rhodium-Based Benzyl C_{sp^3} Nucleophiles. Regioselective rhodium-catalyzed hydrocarboxylation of styrene derivatives and α,β-unsaturated carbonyl compounds was described by the group of Mikami.[30] Use of 1,5-cyclooctadiene (COD) as a ligand and $ZnEt_2$ as an additive afforded α-aryl carboxylic acids in good yields. Moreover, asymmetric induction was successfully achieved in moderate yields with (*S*)-SEGPHOS as a chiral ligand. The proposed catalytic cycle involves transmetalation of an ethyl moiety from $ZnEt_2$ to Rh, followed by β-hydride elimination. Substrate insertion into the Rh−H bond comprises the next step, and its subsequent coupling to CO_2 renders the carboxylated product (Scheme 3).

Scheme 3. Carboxylation Step in the Rh−(*S*)-SEGPHOS-Catalyzed Hydrocarboxylation of Methyl 2-Phenylacrylate[a]

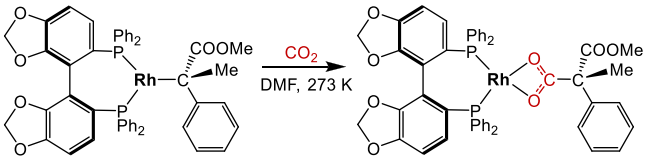

[a]The experimental reaction was originally reported in ref 30.

The Rh−COD-catalyzed hydrocarboxylation was recently investigated by our group.[7] Computational examination of several substrates supported the proposed mechanism but revealed a strong preference for *outer*-sphere CO_2 insertion. Here we analyzed if these findings also apply if COD is exchanged with the diphosphine ligand (*S*)-SEGPHOS (Table S1, reaction 5). Our results for the substrate methyl 2-phenylacrylate support the preference for an *outer*-sphere CO_2 insertion by a margin of 17.0 kcal/mol ($\Delta G^{\ddagger}$ = 15.6 for *outer*-sphere vs 32.6 kcal/mol for *inner*-sphere insertion; Figure 5). As observed in our previous study,[7] the *outer*-sphere TS is characterized by an unusual binding mode of the substrate toward the metal center, with η^6 coordination of the phenyl ring (Figure 5, right). It can be noted that the shown *outer*-sphere TS gives the *S* product, whereas the *R* conformer of the

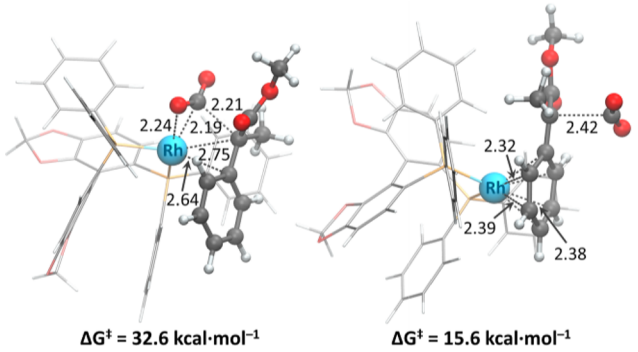

Figure 5. Optimized TSs for *inner*- (left) and *outer*-sphere (right) carboxylation of methyl 2-phenylacrylate with Rh−(*S*)-SEGPHOS (273 K, DMF). Distances are given in Å.

outer-sphere TS is 1.2 kcal/mol higher in energy (Figure S3). The barrier difference corresponds to a computed ee of 80% *S* at 273 K for the studied methyl ester, which is in good agreement with experiments on a related ethyl ester, affording an ee of 60% *S* at 273 K.[30] The agreement supports that the *outer*-sphere TS proposed here is operative for Rh−SEGPHOS-catalyzed carboxylations.

A relevant consideration for all *outer*-sphere TSs is whether the CO_2 molecule at the TS may be able to interact with another component in the reaction mixture, for example a Lewis acid additive.[26] For the Rh−benzyl system, we have previously shown that CO_2 does not interact with the additive $ZnEt_2$.[7] Another possibility may be that CO_2 at the TS interacts with a second Rh complex. We have tested this here for carboxylation of COD−Rh−benzyl. However, the interaction of CO_2 with another Rh complex increases the insertion barrier from 14.4 to 32.4 kcal/mol (273 K, PBE-D2; see the Supporting Information for optimized coordinates and ref 7 for the full computational protocol). This is in line with results indicating that a bimetallic CO_2 insertion mechanism is not beneficial for sterically hindered metal complexes.[71]

Rhodium-Based Alkenyl and Aryl C_{sp^2} Nucleophiles. Carboxylation of aryl- and alkenylboronic esters with Rh in the presence of 1,3-bis(diphenylphosphino)propane (dppp) was described by the group of Iwasawa.[42] The proposed carboxylation mechanism suggests that CO_2 inserts into the rhodium−nucleophile bond (Scheme 4). Kantchev, Qin, and co-workers have studied this reaction using DFT.[33] The results support the suggested mechanism and predict that CO_2 binds to Rh prior to its insertion into the Rh−C bond. With dppp as a ligand, the computed barrier for *inner*-sphere CO_2 insertion was 12.7 kcal/mol (333 K).

Scheme 4. CO_2 Insertion Step in the Rh−dppe-Catalyzed Carboxylation of Arylboronic Esters[a]

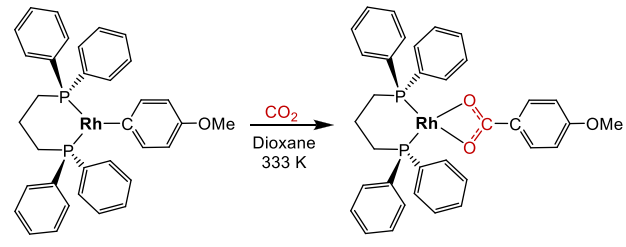

[a]The experimental reaction was originally reported in ref 42.

https://dx.doi.org/10.1021/acs.organomet.0c00090
Organometallics XXXX, XXX, XXX−XXX

We have here used 4-methoxyphenyl and 4-methoxystyrene as *aryl* and *alkenyl* C_{sp^2} nucleophiles, respectively, to revisit the carboxylation step (Table S1, reactions 6a,b). These substrates were experimentally studied by Iwasawa and co-workers, with respectively Rh−(dppp) and Rh−(*p*-MeO-dppp) as catalysts.[42] For both systems, our calculations support that CO_2 coordinates to Rh in a η^2(C,O) mode prior to insertion, forming an energetically low lying adduct. The *inner*-sphere barriers with respect to the adducts are 11.2 kcal/mol (4-methoxyphenyl) and 13.3 kcal/mol (4-methoxystyrene, 333 K; Figure S4). As for the Cu−C_{sp^2} systems above, attempts to obtain *outer*-sphere TSs for these Rh complexes failed, possibly due to geometric and orbital constraints that make an *outer*-sphere insertion inaccessible for C_{sp^2} nucleophiles.

Palladium-Based Benzylic C_{sp^3} Nucleophiles. The group of Iwasawa reported regioselective synthesis of α-branched propionic acid derivatives via Pd−pincer(^{Et}PGeP)-catalyzed hydrocarboxylation of styrenes, using a formate salt as both a reductant and a CO_2 source.[43] The proposed mechanism suggests that the coordination of formate to the palladium catalyst leads to decarboxylation and generation of a hydride species. Insertion of the styrene into the Pd−H bond produces a Pd−benzyl species, which can react with the released CO_2 to give a palladium−carboxylate complex (Scheme 5).

Scheme 5. Carboxylation of a ^{Et}PGeP−Pd−Benzyl Intermediate in the Hydrocarboxylation of a Substituted Styrene[a]

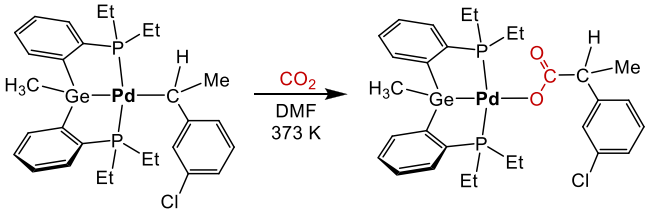

[a]The experimental reaction was originally reported in ref 43.

A DFT study of the Pd-catalyzed carboxylation of unsubstituted styrene has been reported.[35] *Inner*-sphere CO_2 insertion into the Pd−benzyl complex was suggested to be rate-determining; however, an *outer*-sphere path was not considered. Here, we performed a computational evaluation of both the *inner*- and *outer*-sphere pathways for this reaction, employing 3-chlorostyrene as substrate, which is experimentally active, in contrast to unsubstituted styrene.[43] First, we tried to coordinate CO_2 to the Pd complex. However, the relative energy of the adduct is rather high, 38.6 kcal/mol (Figure S5), indicating that CO_2 coordination will not occur. We then optimized the TSs for insertion of CO_2 into the Pd−benzyl bond. Interestingly, for our model, *outer*-sphere CO_2 insertion is preferred by 7.2 kcal/mol ($\Delta G^{\ddagger}$ = 19.8 kcal/mol for *outer*-sphere vs $\Delta G^{\ddagger}$ = 27.0 kcal/mol for *inner*-sphere, 373 K, Figure 6). The geometry around the Ge−Me moiety in the preferred conformations of the two TSs is worth noting. Whereas the *outer*-sphere insertion TS minimizes the steric hindrance between Ge−Me and 3-chlorostyrene, the *inner*-sphere TS reduces the repulsion between Ge−Me and CO_2 (Figure 6). At the *outer*-sphere TS, the benzylic nucleophile coordinates in an η^2 mode to Pd, in contrast to the η^1 interaction at the *inner*-sphere TS. Indeed, a pattern is seen

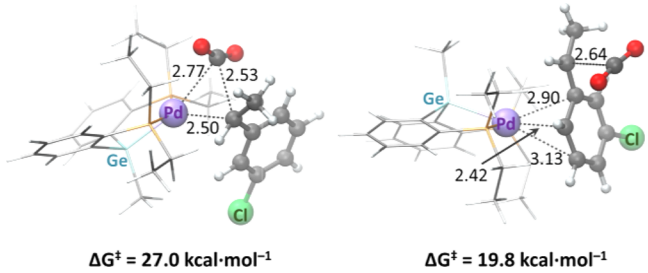

Figure 6. Optimized TSs for *inner*- (left) and *outer*-sphere (right) carboxylation of 3-chlorostyrene with a ^{Et}PGeP−Pd complex (DMF, 373 K). Distances are given in Å.

for all metal−benzyl complexes studied here, where *outer*-sphere TSs show more interactions between the metal and nucleophile (η^2, η^3, or η^6 binding) in comparison to *inner*-sphere TSs (η^1 or η^2, Figures 3, 5, and 6). The stronger substrate coordination may be contributing to lower the energy of the *outer*-sphere TS.

The combined results for the Pd−, Rh−, and Cu−benzyl systems studied here indicate that *outer*-sphere CO_2 insertion in many cases may be preferred for metal−benzyl complexes or, at minimum, may be competitive with *inner*-sphere insertion. This conclusion is in contrast with previous studies reporting *inner*-sphere CO_2 insertion for Pd and Cu with benzylic nucleophiles.[35,36,65]

Palladium-Based Alkenyl C_{sp^2} Nucleophiles. There appear to be few reported carboxylations of Pd−alkenyl systems; however, the group of Iwasawa has reported one such reaction, involving activation of a vinylic C−H bond of 2-hydroxystyrenes (Table S1, reaction 8).[44] The isolated X-ray structure of a key Pd−alkenyl intermediate showed that two substrates coordinate to the metal: one of them acts as a neutral ligand, whereas the other has undergone C−H activation to become an alkenyl (Figure 7). The OH groups

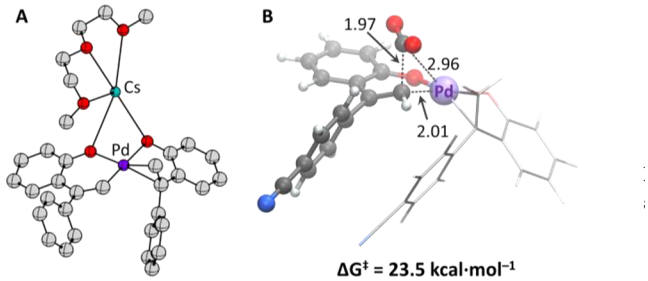

Figure 7. (A) Reported X-ray structure of a Pd−alkenyl complex formed from $H_2C{=}CRR'$, where R = 2-hydroxyphenyl and R′ = phenyl.[44] Cs is coordinated by diglyme solvent. (B) CO_2 insertion TS computed here for a related Pd−alkenyl species (see main text).

of both substrates are deprotonated and coordinated to Pd, as well as to a Cs counterion present in solution. Here we studied the carboxylation of the Pd−alkenyl complex formed from the substrate that performed best in the reported experiments, $H_2C{=}CRR'$, where R = 2-hydroxyphenyl and R′ = 4-cyanophenyl.[44] The computations (which were performed without Cs present[72]) lead to the identification of a single TS, with a barrier of 23.5 kcal/mol (Figure 7). Analysis of the geometry revealed a Pd−C_{CO_2} distance of 2.96 Å, which appears significantly longer than the metal−C_{CO_2} distances found for other C_{sp^2} carboxylation TSs computed here (up to

https://dx.doi.org/10.1021/acs.organomet.0c00090
Organometallics XXXX, XXX, XXX−XXX

2.20 Å for Rh−C_{sp^2} TSs and up to 2.70 Å for Cu−C_{sp^2} TSs, Table S2).

In order to evaluate if the long metal−C_{CO_2} distance is a general feature of CO_2 insertion into Pd−C_{sp^2} bonds, we designed four virtual alkenyl systems on the basis of experimentally known Pd−pincer complexes (for optimized TS geometries see Figures S6−S9). In all cases, the alkenyl nucleophile was derived from 1-phenyl-1-propyne, in analogy to the Cu−C_{sp^2} system studied above (Scheme 2). The first virtual Pd−C_{sp^2} complex is based on the experimentally known ^{Et}PGeP ligand (used in the carboxylation of styrene derivatives[43]), which also was employed in the Pd−C_{sp^3} case above (Scheme 5). The Pd−C_{CO_2} distance of 2.74 Å at the carboxylation TS is the shortest computed here for a Pd−C_{sp^2} complex (Figure 8), which may be due to the flexible Et

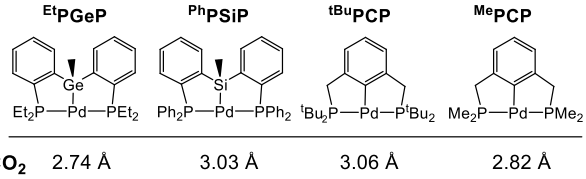

Figure 8. Pd−CO_2 distances at the carboxylation TS of pincer Pd−alkenyl complexes (for optimized geometries see Figures S6−S9).

substituents. The second virtual Pd−C_{sp^2} complex features the experimentally known ^{Ph}PSiP ligand, which has been used in allene carboxylations.[73] The congestion caused by the Ph substituents repulses the approaching CO_2, resulting in a metal−C_{CO_2} distance of 3.03 Å. The third virtual Pd−C_{sp^2} complex features the experimentally known ^{tBu}PCP ligand (used in carboxylation of Pd−allyl and −methyl groups).[10] The ^{t}Bu substituents on this complex do not allow a close approach of CO_2, which results in a metal−C_{CO_2} distance of 3.06 Å, the longest computed here (Figure 8). Out of curiosity, we made a fourth complex, where the tBu groups were truncated to methyl groups to reduce steric hindrance. In comparison to ^{tBu}PCP, the metal−C_{CO_2} distance for the ^{Me}PCP complex is shorter but remains as much as 2.82 Å (Figure 8).

We did not study an experimental Pd−aryl case here, such as the seminal Pd-catalyzed carboxylation of aryl-bromides reported by Martin and co-workers,[74] due to the size and complexity of the ligand that was used. However, for comparison to the alkenyl case, we computationally studied a ^{tBu}PCP−Pd−phenyl complex (Figure S10). The obtained carboxylation TS shows a Pd−C_{CO_2} distance of 2.97 Å, similar to those for the Pd−alkenyl systems (Figure 8). However, the computed barrier of 41.7 kcal/mol (298 K) indicates that this complex may not be reactive, in line with results by Wendt and co-workers.[75]

It can be concluded that the six optimized Pd−C_{sp^2} TSs show similar geometric features: for example, O=C=O angles of 143−149° and metal−C_{CO_2} distances of 2.82−3.06 Å (Table 1). However, a question is how these TSs should be classified. Table 1 shows that there is relatively poor similarity to *outer*-sphere TSs computed here but better similarity to other *inner*-sphere TSs. We conclude that the Pd−C_{sp^2} TSs may be classified as *inner*-sphere, despite the relatively long metal−C_{CO_2} distances. It needs to be kept in mind that all Pd−C_{sp^2} complexes discussed here have fully saturated coordination spheres, with four ligands prior to insertion of CO_2, which may explain the low propensity of the metal to interact with CO_2. Therefore, the results for less coordinated Pd species may differ. For example, in the reported geometry for a Pd-catalyzed decarboxylation of aryls, the complex has three ligands in addition to CO_2, which allows for a smaller Pd−C_{CO_2} distance (2.58 Å) and a pronounced Pd−O_{CO_2} interaction (2.05 Å),[37] not observed in any of the Pd complexes studied here.

Table 1. Range of Selected Geometric Parameters for *Inner*- and *Outer*-Sphere CO_2 Insertion TSs in Comparison to Pd−C_{sp^2} Systems

	O=C=O (deg)	C_{CO_2}−C_{Nu}−M (deg)[a]	M−C_{CO_2} (Å)[a]
outer-sphere TSs[b]	147−163	124−146	4.04−5.93
inner-sphere TSs[c]	138−152	51−82	2.16−2.76
Pd−C_{sp^2} TSs[d]	143−149	75−96	2.82−3.06

[a]M = metal. [b]Based on 8 *outer*-sphere TSs in Table S2, [c]Based on 11 *inner*-sphere TSs in Table S2, not including Pd−C_{sp^2}. [d]Based on 6 Pd−C_{sp^2} TSs in Table S2.

CONCLUSIONS

The mechanistic details of transition metal-catalyzed C−CO_2 bond formations were computationally examined for a series of experimentally reported Cu, Rh, and Pd systems involving C_{sp^3} *benzyl* and C_{sp^2} *alkenyl* or *aryl* nucleophiles.

For benzylic C_{sp^3} nucleophiles, we show that the studied Pd− and Rh−benzyl complexes strongly favor *outer*-sphere CO_2 insertion. The *outer*-sphere TSs reduce sterics between CO_2 and the metal ligands and allow for stronger coordination of the benzylic substrates to the metal, which may contribute to the observed preference for *outer*-sphere insertion. For four studied Cu−benzyl complexes, our results indicate that large NHC ligands promote a slight preference for *outer*-sphere paths, but as the ligand is reduced, *inner*-sphere insertion becomes equally accessible and eventually favored. Several previous DFT studies reported only *inner*-sphere insertion for carboxylation of Cu− and Pd−benzyl complexes,[35,36,65] but our study of these complexes shows that *outer*-sphere insertion is equal or lower in barrier. These results highlight that *outer*-sphere pathways need to be included in mechanistic studies of metal−benzyl carboxylations.

For 11 experimental and virtual metal−C_{sp^2} complexes based on Cu, Rh, and Pd, our results suggest that CO_2 insertion occurs via an *inner*-sphere pathway, which is in line with previous computational results on Cu− and Rh−C_{sp^2} systems.[21,32−34] For a series of Pd−alkenyl complexes, we show that the CO_2 insertion TSs feature rather weak Pd−CO_2 interactions; however, these TSs should nonetheless be classified as *inner*-sphere.

It has to be kept in mind that our conclusions may be valid only for the studied complexes: e.g., Cu−NHCs, Rh−diphosphine and Rh−dialkenes, and Pd−pincer and Pd−alkoxide complexes. Further studies are needed to show if the mechanistic trends observed here are universal for carboxylation reactions involving late transition metals.

https://dx.doi.org/10.1021/acs.organomet.0c00090
Organometallics XXXX, XXX, XXX−XXX

■ ASSOCIATED CONTENT

Supporting Information

The Supporting Information is available free of charge at https://pubs.acs.org/doi/10.1021/acs.organomet.0c00090.

Overview of the studied reactions and additional geometrical parameters and figures of computed TSs (PDF)

Optimized coordinates (XYZ)

■ AUTHOR INFORMATION

Corresponding Author

Kathrin H. Hopmann − *Hylleraas Centre for Quantum Molecular Sciences, Department of Chemistry, UiT The Arctic University of Norway, N-9037 Tromsø, Norway;* orcid.org/0000-0003-2798-716X; Email: kathrin.hopmann@uit.no

Authors

Diego García-López − *Hylleraas Centre for Quantum Molecular Sciences, Department of Chemistry, UiT The Arctic University of Norway, N-9037 Tromsø, Norway*

Ljiljana Pavlovic − *Hylleraas Centre for Quantum Molecular Sciences, Department of Chemistry, UiT The Arctic University of Norway, N-9037 Tromsø, Norway*

Complete contact information is available at: https://pubs.acs.org/10.1021/acs.organomet.0c00090

Notes

The authors declare no competing financial interest.

■ ACKNOWLEDGMENTS

This work has been supported by the Research Council of Norway (Centre of Excellence Grant No. 262695), by the Tromsø Research Foundation (Grant No. TFS2016KHH), by NordForsk (Grant No. 85378), and by Notur-The Norwegian Metacenter for Computational Science through grants of computer time (Nos. nn9330k and nn4654k).

■ REFERENCES

(1) Cokoja, M.; Bruckmeier, C.; Rieger, B.; Herrmann, W. A.; Kühn, F. E. Transformation of Carbon Dioxide with Homogeneous Transition-Metal Catalysts: A Molecular Solution to a Global Challenge? *Angew. Chem., Int. Ed.* **2011**, *50*, 8510−8537.

(2) Tortajada, A.; Juliá-Hernández, F.; Börjesson, M.; Moragas, T.; Martin, R. Transition-Metal-Catalyzed Carboxylation Reactions with Carbon Dioxide. *Angew. Chem., Int. Ed.* **2018**, *57*, 15948−15982.

(3) Dabral, S.; Schaub, T. The Use of Carbon Dioxide (CO_2) as a Building Block in Organic Synthesis from an Industrial Perspective. *Adv. Synth. Catal.* **2019**, *361*, 223−246.

(4) Yang, Y.; Lee, J.-W. Toward Ideal Carbon Dioxide Functionalization. *Chem. Sci.* **2019**, *10*, 3905−3926.

(5) Darensbourg, D. J. Chemistry of Carbon Dioxide Relevant to Its Utilization: A Personal Perspective. *Inorg. Chem.* **2010**, *49*, 10765−10780.

(6) Vaitla, J.; Guttormsen, Y.; Mannisto, J. K.; Nova, A.; Repo, T.; Bayer, A.; Hopmann, K. H. Enantioselective Incorporation of CO_2: Status and Potential. *ACS Catal.* **2017**, *7*, 7231−7244.

(7) Pavlovic, Lj.; Vaitla, J.; Bayer, A.; Hopmann, K. H. Rhodium-Catalyzed Hydrocarboxylation: Mechanistic Analysis Reveals Unusual Transition State for Carbon−Carbon Bond Formation. *Organometallics* **2018**, *37*, 941−948.

(8) Vummaleti, S. V. C.; Talarico, G.; Nolan, S. P.; Cavallo, L.; Poater, A. How Easy Is CO_2 Fixation by M−C Bond Containing Complexes (M = Cu, Ni, Co, Rh, Ir)? *Org. Chem. Front.* **2016**, *3*, 19−23.

(9) Lau, K.-C.; Petro, B. J.; Bontemps, S.; Jordan, R. F. Comparative Reactivity of Zr− and Pd−Alkyl Complexes with Carbon Dioxide. *Organometallics* **2013**, *32*, 6895−6898.

(10) Johnson, M. T.; Johansson, R.; Kondrashov, M. V.; Steyl, G.; Ahlquist, M. S. G.; Roodt, A.; Wendt, O. F. Mechanisms of the CO_2 Insertion into (PCP) Palladium Allyl and Methyl σ-Bonds. A Kinetic and Computational Study. *Organometallics* **2010**, *29*, 3521−3529.

(11) Schmeier, T. J.; Hazari, N.; Incarvito, C. D.; Raskatov, J. A. Exploring the Reactions of CO_2 with PCP Supported Nickel Complexes. *Chem. Commun.* **2011**, *47*, 1824−1826.

(12) Fan, T.; Chen, X.; Lin, Z. Theoretical Studies of Reactions of Carbon Dioxide Mediated and Catalysed by Transition Metal Complexes. *Chem. Commun.* **2012**, *48*, 10808−10828.

(13) Vummaleti, S. V. C.; Talarico, G.; Nolan, S. P.; Cavallo, L.; Poater, A. Mechanism of CO_2 Fixation by Ir^{I}−X Bonds (X = OH, OR, N, C). *Eur. J. Inorg. Chem.* **2015**, *2015*, 4653−4657.

(14) Sayyed, F. B.; Tsuji, Y.; Sakaki, S. The Crucial Role of a Ni(I) Intermediate in Ni-Catalyzed Carboxylation of Aryl Chloride with CO_2: A Theoretical Study. *Chem. Commun.* **2013**, *49*, 10715−10717.

(15) Jover, J.; Maseras, F. Computational Characterization of the Mechanism for Coinage-Metal-Catalyzed Carboxylation of Terminal Alkynes. *J. Org. Chem.* **2014**, *79*, 11981−11987.

(16) Yang, L.; Yuan, Y.; Wang, H.; Zhang, N.; Hong, S. Theoretical Insights into Copper(I)−NHC-Catalyzed C−H Carboxylation of Terminal Alkynes with CO_2: The Reaction Mechanisms and the Roles of NHC. *RSC Adv.* **2014**, *4*, 32457−32466.

(17) Yuan, R.; Lin, Z. Mechanism for the Carboxylative Coupling Reaction of a Terminal Alkyne, CO_2, and an Allylic Chloride Catalyzed by the Cu(I) Complex: A DFT Study. *ACS Catal.* **2014**, *4*, 4466−4473.

(18) Ostapowicz, T. G.; Hölscher, M.; Leitner, W. CO_2 Insertion into Metal−Carbon Bonds: A Computational Study of Rh^{I} Pincer Complexes. *Chem. - Eur. J.* **2011**, *17*, 10329−10338.

(19) Ostapowicz, T. G.; Hölscher, M.; Leitner, W. Catalytic Hydrocarboxylation of Olefins with CO_2 and H_2 − a DFT Computational Analysis. *Eur. J. Inorg. Chem.* **2012**, *2012*, 5632−5641.

(20) Schmeier, T. J.; Nova, A.; Hazari, N.; Maseras, F. Synthesis of PCP-Supported Nickel Complexes and Their Reactivity with Carbon Dioxide. *Chem. - Eur. J.* **2012**, *18*, 6915−6927.

(21) Fan, T.; Sheong, F. K.; Lin, Z. DFT Studies on Copper-Catalyzed Hydrocarboxylation of Alkynes Using CO_2 and Hydrosilanes. *Organometallics* **2013**, *32*, 5224−5230.

(22) Wang, Q.; Guo, C.-H.; Ren, Y.; Wu, H.-S. A Computational Study on the Insertion of CO_2 into (PSiP)Palladium Allyl σ-Bond. *J. Mol. Model.* **2015**, *21*, 122.

(23) Obst, M.; Pavlovic, Lj.; Hopmann, K. H. Carbon-Carbon Bonds with CO_2: Insights from Computational Studies. *J. Organomet. Chem.* **2018**, *864*, 115−127.

(24) Hazari, N.; Heimann, J. E. Carbon Dioxide Insertion into Group 9 and 10 Metal−Element σ Bonds. *Inorg. Chem.* **2017**, *56*, 13655−13678.

(25) Leitner, W. The Coordination Chemistry of Carbon Dioxide and Its Relevance for Catalysis: A Critical Survey. *Coord. Chem. Rev.* **1996**, *153*, 257−284.

(26) Heimann, J. E.; Bernskoetter, W. H.; Hazari, N.; Mayer, J. M. Acceleration of CO_2 Insertion into Metal Hydrides: Ligand, Lewis Acid, and Solvent Effects on Reaction Kinetics. *Chem. Sci.* **2018**, *9*, 6629−6638.

(27) Takimoto, M.; Nakamura, Y.; Kimura, K.; Mori, M. Highly Enantioselective Catalytic Carbon Dioxide Incorporation Reaction: Nickel-Catalyzed Asymmetric Carboxylative Cyclization of Bis-1,3-Dienes. *J. Am. Chem. Soc.* **2004**, *126*, 5956−5957.

(28) Dian, L.; Müller, D. S.; Marek, I. Asymmetric Copper-Catalyzed Carbomagnesiation of Cyclopropenes. *Angew. Chem., Int. Ed.* **2017**, *56*, 6783−6787.

(29) Gui, Y.-Y.; Hu, N.; Chen, X.-W.; Liao, L.; Ju, T.; Ye, J.-H.; Zhang, Z.; Li, J.; Yu, D.-G. Highly Regio- and Enantioselective Copper-Catalyzed Reductive Hydroxymethylation of Styrenes and 1,3-Dienes with CO_2. *J. Am. Chem. Soc.* **2017**, *139*, 17011−17014.

(30) Kawashima, S.; Aikawa, K.; Mikami, K. Rhodium-Catalyzed Hydrocarboxylation of Olefins with Carbon Dioxide. *Eur. J. Org. Chem.* **2016**, *2016*, 3166−3170.
(31) Xue, L.; Su, W.; Lin, Z. Mechanism of Silver- and Copper-Catalyzed Decarboxylation Reactions of Aryl Carboxylic Acids. *Dalton Trans.* **2011**, *40*, 11926−11936.
(32) Dang, L.; Lin, Z.; Marder, T. B. DFT Studies on the Carboxylation of Arylboronate Esters with CO_2 Catalyzed by Copper(I) Complexes. *Organometallics* **2010**, *29*, 917−927.
(33) Qin, H.-L.; Han, J.-B.; Hao, J.-H.; Kantchev, E. A. B. Computational and Experimental Comparison of Diphosphane and Diene Ligands in the Rh-Catalysed Carboxylation of Organoboron Compounds with CO_2. *Green Chem.* **2014**, *16*, 3224−3229.
(34) Wang, Q.; Jia, J.-F.; Guo, C.-H.; Wu, H.-S. Mechanistic Investigation of Cu(I)-Mediated Three-Component Domino Reaction of Asymmetrical Alkynes with Carbon Dioxide: Theoretical Rationale for the Regioselectivity. *J. Organomet. Chem.* **2013**, *748*, 84−88.
(35) Lv, X.; Huang, F.; Wu, Y.-B.; Lu, G. Origin of Ligand Effects on Reactivities of Pincer-Pd Catalyzed Hydrocarboxylation of Allenes and Alkenes with Formate Salts: A Computational Study. *Catal. Sci. Technol.* **2018**, *8*, 2835−2840.
(36) Lin, S.; Lin, Z. DFT Studies on the Mechanism of Copper-Catalyzed Boracarboxylation of Alkene with CO_2 and Diboron. *Organometallics* **2019**, *38*, 240−247.
(37) Xue, L.; Su, W.; Lin, Z. A DFT Study on the Pd-Mediated Decarboxylation Process of Aryl Carboxylic Acids. *Dalton Trans.* **2010**, *39*, 9815−9822.
(38) Butcher, T. W.; McClain, E. J.; Hamilton, T. G.; Perrone, T. M.; Kroner, K. M.; Donohoe, G. C.; Akhmedov, N. G.; Petersen, J. L.; Popp, B. V. Regioselective Copper-Catalyzed Boracarboxylation of Vinyl Arenes. *Org. Lett.* **2016**, *18*, 6428−6431.
(39) Juhl, M.; Laursen, S. L. R.; Huang, Y.; Nielsen, D. U.; Daasbjerg, K.; Skrydstrup, T. Copper-Catalyzed Carboxylation of Hydroborated Disubstituted Alkenes and Terminal Alkynes with Cesium Fluoride. *ACS Catal.* **2017**, *7*, 1392−1396.
(40) Fujihara, T.; Xu, T.; Semba, K.; Terao, J.; Tsuji, Y. Copper-Catalyzed Hydrocarboxylation of Alkynes Using Carbon Dioxide and Hydrosilanes. *Angew. Chem., Int. Ed.* **2011**, *50*, 523−527.
(41) Ohishi, T.; Nishiura, M.; Hou, Z. Carboxylation of Organoboronic Esters Catalyzed by N-Heterocyclic Carbene Copper(I) Complexes. *Angew. Chem., Int. Ed.* **2008**, *47*, 5792−5795.
(42) Ukai, K.; Aoki, M.; Takaya, J.; Iwasawa, N. Rhodium(I)-Catalyzed Carboxylation of Aryl- and Alkenylboronic Esters with CO_2. *J. Am. Chem. Soc.* **2006**, *128*, 8706−8707.
(43) Takaya, J.; Miyama, K.; Zhu, C.; Iwasawa, N. Metallic Reductant-Free Synthesis of α-Substituted Propionic Acid Derivatives through Hydrocarboxylation of Alkenes with a Formate Salt. *Chem. Commun.* **2017**, *53*, 3982−3985.
(44) Sasano, K.; Takaya, J.; Iwasawa, N. Palladium(II)-Catalyzed Direct Carboxylation of Alkenyl C−H Bonds with CO_2. *J. Am. Chem. Soc.* **2013**, *135*, 10954−10957.
(45) Parr, R. G.; Yang, W. *Density Functional Theory of Atoms and Molecules*; Oxford University Press: 1989.
(46) Frisch, M. J.; Trucks, G. W.; Schlegel, H. B.; Scuseria, G. E.; Robb, M. A.; Cheeseman, J. R.; Scalmani, G.; Barone, V.; Mennucci, B.; Petersson, G. A.; Nakatsuji, H.; Caricato, M.; Li, X.; Hratchian, H. P.; Izmaylov, A. F.; Bloino, J.; Zheng, G.; Sonnenberg, J. L.; Hada, M.; Ehara, M.; Toyota, K.; Fukuda, R.; Hasegawa, J.; Ishida, M.; Nakajima, T.; Honda, Y.; Kitao, O.; Nakai, H.; Vreven, T.; Montgomery, J. A., Jr.; Peralta, J. E.; Ogliaro, F.; Bearpark, M.; Heyd, J. J.; Brothers, E.; Kudin, K. N.; Staroverov, V. N.; Kobayashi, R.; Normand, J.; Raghavachari, K.; Rendell, A.; Burant, J. C.; Iyengar, S. S.; Tomasi, J.; Cossi, M.; Rega, N.; Millam, J. M.; Klene, M.; Knox, J. E.; Cross, J. B.; Bakken, V.; Adamo, C.; Jaramillo, J.; Gomperts, R.; Stratmann, R. E.; Yazyev, O.; Austin, A. J.; Cammi, R.; Pomelli, C.; Ochterski, J. W.; Martin, R. L.; Morokuma, K.; Zakrzewski, V. G.; Voth, G. A.; Salvador, P.; Dannenberg, J. J.; Dapprich, S.; Daniels, A. D.; Farkas, O.; Foresman, J. B.; Ortiz, J. V.; Cioslowski, J.; Fox, D. J. *Gaussian 09, rev. D.01*; Gaussian, Inc.: Wallingford, CT, 2013.
(47) Becke, A. D. Density-functional Thermochemistry. III. The Role of Exact Exchange. *J. Chem. Phys.* **1993**, *98*, 5648−5652.
(48) Lee, C.; Yang, W.; Parr, R. G. Development of the Colle-Salvetti Correlation-Energy Formula into a Functional of the Electron Density. *Phys. Rev. B: Condens. Matter Mater. Phys.* **1988**, *37*, 785−789.
(49) Grimme, S.; Antony, J.; Ehrlich, S.; Krieg, H. A Consistent and Accurate Ab Initio Parametrization of Density Functional Dispersion Correction (DFT-D) for the 94 Elements H-Pu. *J. Chem. Phys.* **2010**, *132*, 154104−154119.
(50) Grimme, S.; Ehrlich, S.; Goerigk, L. Effect of the Damping Function in Dispersion Corrected Density Functional Theory. *J. Comput. Chem.* **2011**, *32*, 1456−1465.
(51) Scalmani, G.; Frisch, M. J. Continuous Surface Charge Polarizable Continuum Models of Solvation. I. General Formalism. *J. Chem. Phys.* **2010**, *132*, 114110−114115.
(52) Dolg, M.; Wedig, U.; Stoll, H.; Preuss, H. Energy-adjusted Ab Initio Pseudopotentials for the First Row Transition Elements. *J. Chem. Phys.* **1987**, *86*, 866−872.
(53) Andrae, D.; Häußermann, U.; Dolg, M.; Stoll, H.; Preuß, H. Energy-adjusted *ab initio* pseudopotentials for the second and third row transition elements. *Theor. Chim. Acta* **1990**, *77*, 123−141.
(54) Ditchfield, R.; Hehre, W. J.; Pople, J. A. Self-Consistent Molecular-Orbital Methods. IX. An Extended Gaussian-Type Basis for Molecular-Orbital Studies of Organic Molecules. *J. Chem. Phys.* **1971**, *54*, 724−728.
(55) Hehre, W. J.; Ditchfield, R.; Pople, J. A. Self-Consistent Molecular Orbital Methods. *J. Chem. Phys.* **1972**, *56*, 2257−2261.
(56) Dill, J. D.; Pople, J. A. Self-consistent Molecular Orbital Methods. XV. Extended Gaussian-type Basis Sets for Lithium, Beryllium, and Boron. *J. Chem. Phys.* **1975**, *62*, 2921−2923.
(57) Francl, M. M.; Pietro, W. J.; Hehre, W. J.; Binkley, J. S.; Gordon, M. S.; DeFrees, D. J.; Pople, J. A. Self-consistent Molecular Orbital Methods. XXIII. A Polarization-type Basis Set for Second-row Elements. *J. Chem. Phys.* **1982**, *77*, 3654−3665.
(58) Rassolov, V. A.; Ratner, M. A.; Pople, J. A.; Redfern, P. C.; Curtiss, L. A. 6-31G* Basis Set for Third-Row Atoms. *J. Comput. Chem.* **2001**, *22*, 976−984.
(59) Spitznagel, G. W.; Clark, T.; von Ragué Schleyer, P.; Hehre, W. J. An Evaluation of the Performance of Diffuse Function-Augmented Basis Sets for Second Row Elements, Na-Cl. *J. Comput. Chem.* **1987**, *8*, 1109−1116.
(60) Krishnan, R.; Binkley, J. S.; Seeger, R.; Pople, J. A. Self-consistent Molecular Orbital Methods. XX. A Basis Set for Correlated Wave Functions. *J. Chem. Phys.* **1980**, *72*, 650−654.
(61) McLean, A. D.; Chandler, G. S. Contracted Gaussian Basis Sets for Molecular Calculations. I. Second Row Atoms, Z = 11−18. *J. Chem. Phys.* **1980**, *72*, 5639−5648.
(62) Ehlers, A. W.; Böhme, M.; Dapprich, S.; Gobbi, A.; Höllwarth, A.; Jonas, V.; Köhler, K. F.; Stegmann, R.; Veldkamp, A.; Frenking, G. A Set of F-Polarization Functions for Pseudo-Potential Basis Sets of the Transition Metals Sc-Cu, Y-Ag and La-Au. *Chem. Phys. Lett.* **1993**, *208*, 111−114.
(63) Zhang, L.; Cheng, J.; Carry, B.; Hou, Z. Catalytic Boracarboxylation of Alkynes with Diborane and Carbon Dioxide by an N-Heterocyclic Carbene Copper Catalyst. *J. Am. Chem. Soc.* **2012**, *134*, 14314−14317.
(64) Carry, B.; Zhang, L.; Nishiura, M.; Hou, Z. Synthesis of Lithium Boracarbonate Ion Pairs by Copper-Catalyzed Multi-Component Coupling of Carbon Dioxide, Diboron, and Aldehydes. *Angew. Chem., Int. Ed.* **2016**, *55*, 6257−6260.
(65) Lv, X.; Wu, Y.-B.; Lu, G. Computational Exploration of Ligand Effects in Copper-Catalyzed Boracarboxylation of Styrene with CO_2. *Catal. Sci. Technol.* **2017**, *7*, 5049−5054.
(66) Huynh, H. V. Electronic Properties of N-Heterocyclic Carbenes and Their Experimental Determination. *Chem. Rev.* **2018**, *118*, 9457−9492.

https://dx.doi.org/10.1021/acs.organomet.0c00090
Organometallics XXXX, XXX, XXX−XXX

(67) Obst, M. F.; Gevorgyan, A.; Bayer, A.; Hopmann, K. H. Mechanistic Insights into Copper-Catalyzed Carboxylations. *Organometallics* **2020**, DOI: 10.1021/acs.organomet.9b00710.
(68) The ee estimate assumes that only one diastereomeric intermediate is formed and that it will react via *inner*- and *outer*-sphere CO_2 insertion (giving opposite configurations) with an energy difference of 1 kcal/mol between the two TSs. However, normally two diastereomeric intermediates are formed in an asymmetric reaction, and each one may react via both *inner*- and *outer*-sphere carboxylation. Thus, the ee for chiral NHCs would be determined by four TSs, not two. Here we have only computed achiral NHCs and can thus only present an estimate based on two TSs.
(69) With Cl_2IPr as ligand, this substrate provided a 75:25 mixture of regioisomers in experiment,[40] with the major regioisomer exhibiting carboxylation at the phenyl-substituted carbon. The TSs studied here correspond to formation of the major regioisomer.
(70) Ryu, H.; Park, J.; Kim, H. K.; Park, J. Y.; Kim, S.-T.; Baik, M.-H. Pitfalls in Computational Modeling of Chemical Reactions and How To Avoid Them. *Organometallics* **2018**, *37*, 3228−3239.
(71) Arayachukiat, S.; Yingcharoen, P.; Vummaleti, S. V. C.; Cavallo, L.; Poater, A.; Elia, V. D. Cycloaddition of CO_2 to Challenging *N*-Tosyl Aziridines Using a Halogen-Free Niobium Complex: Catalytic Activity and Mechanistic Insights. *Mol. Catal.* **2017**, *443*, 280−285.
(72) Geometry optimizations of a computational model involving Cs and diglyme solvent coordinated to the alkoxide groups (as shown in the X-ray structure, Figure 7) did not converge properly, and Cs and diglyme therefore had to be removed from the model.
(73) Takaya, J.; Iwasawa, N. Hydrocarboxylation of Allenes with CO_2 Catalyzed by Silyl Pincer-Type Palladium Complex. *J. Am. Chem. Soc.* **2008**, *130*, 15254−15255.
(74) Correa, A.; Martín, R. Palladium-catalyzed direct carboxylation of aryl bromides with carbon dioxide. *J. Am. Chem. Soc.* **2009**, *131*, 15974−15975.
(75) Johansson, R.; Jarenmark, M.; Wendt, O. F. Insertion of Carbon Dioxide into (PCP)Pd^{II}−Me Bonds. *Organometallics* **2005**, *24*, 4500−4502.

https://dx.doi.org/10.1021/acs.organomet.0c00090
Organometallics XXXX, XXX, XXX−XXX